Materials Research Proceedings 41 (2024) 1732-1740 https://doi.org/10.21741/9781644903131-192

On the impact welding of dissimilar alloys for use in multimaterial skeletal fixation devices

SANGUEDOLCE Michela[1,a *], ABDELMAOLA Mohammed[2,b], BORDA Francesco[1,c], CHO Dae Hyun[2,d], AVEY Thomas[2,e], OLIVAS-ALANIS Luis H.[2,f], CHMIELEWSKA Agnieszka[2,g], VIVEK Anupam[2,h], DAEHN Glenn[2,i], LUO Alan A.[2,l], PANTON Boyd[2,m], FILICE Luigino[1,n] and DEAN David[2,3,o]

[1]Dept. of Mechanical, Energy and Management Engineering, University of Calabria, Rende, CS, Italy

[2]Dept. of Materials Science and Engineering, The Ohio State University, Columbus, OH, USA

[3]Dept. of Plastic and Reconstructive Surgery, The Ohio State University, Columbus, OH, USA

[a]michela.sanguedolce@unical.it, [b]abdelmaola.1@osu.edu, [c]francesco.borda@unical.it, [d]cho.1151@osu.edu, [e]avey.13@osu.edu, [f]olivas.11@osu.edu, [g]achmielewska00@gmail.com, [h]vivek.5@osu.edu, [i]daehn.1@osu.edu, [l]luo.445@osu.edu, [m]panton.7@osu.edu, [n]luigino.filice@unical.it, [o]david.dean@osumc.edu

Keywords: Finite Element Analysis, Impact Welding, Dissimilar Welding, NiTi Alloys, Mg Alloys, Skeletal Fixation

Abstract. Multi-material skeletal fixators appear to be a promising approach to reduce failure due to the high stiffness of standard-of-care fixators. Nevertheless, joining different materials is challenging due to their different properties. High-velocity impact welding, a solid-state welding process, involves the collision of a "flyer" (moving) part with a stationary "target" at very high speed (i.e., hundreds of meters per second). In this paper we present a preliminary experimental campaign to use laser impact welding to join *NiTi* and *Mg* alloy *Mg-1.2Zn-0.5Ca-0.5Mn* (wt%) sheets and the parallel development of a finite element model to allow gathering further insights into the complex phenomena involved in the process. Preliminary results show the deposition of the *Mg* alloy on *NiTi* sheets by tuning the joining process conditions and promising results of the numerical model in terms of accordance with experiments: these findings provide the basis for further process optimization, numerical model calibration and the application of a valid protocol for multi-material skeletal fixation devices.

Introduction

Excessively stiff skeletal fixators are well known to interrupt physiological loading patterns of the contacting bone, bringing to the stress shielding phenomenon and early device failure, which hinders patients' quality of life [1]. The choice of materials with lower stiffness able to restore the physiological loading patterns into bone, as compared to the current and overly stiff gold standard *Ti6Al4V* alloy, represents a viable strategy to prevent these phenomena from occurring. Attempts to develop multi-material skeletal fixators are of current interest in this research field [2], including patent applications [3].Within the investigated materials, *NiTi* alloys and *Mg* alloys play a major role due to the superelasticity and lower stiffness of the former - compared to the current standard of care alloys - and the resorbability of the latter.

A critical step in the design of these multi-material devices is the joining. Friction stir processes have been successfully employed to obtain *NiTi – Mg* alloy composites [4] and welds [5]. However, the current configuration of the process constraints the size of the parts that can be obtained, although micro-level friction stir processing is currently being studied [6]. Furthermore,

these alloys have extremely different physical and metallurgical properties, thus a good quality joint is difficult to obtain without compromising the materials' properties [7].

High-velocity impact welding, within the solid-state welding processes, involves the high-speed collision (100 – 1000 m/s [8]) of a flyer part onto a target part generating a jet able to clean and expose non-contaminated surfaces to obtain metallurgical bonding. It represents a viable solution to obtain dissimilar welding on the millimeter/micron-scale and, within a defined weldability window, preventing the formation of poor quality intermetallic compounds at the weld interface, due to the low welding temperatures involved and the fast welding speed [9]. Impact welding can be implemented on different length scales using different means to accelerate the flyer, depending on the size of the parts to be welded [8].

The possibility to obtain dissimilar welding of *NiTi* without affecting its superelasticity was demonstrated by using solid-state welding processes like Vaporizing Foil Actuator Welding [10] and Laser Impact Welding, by properly selecting processing conditions [11].

Laser impact welding (LIW), as a collision welding process, involves a moving part (flyer) launched towards a stationary part (target) following the formation of an expanding plasma. Plasma is generated by the vaporization of a sacrificial ablative layer and confined into a properly selected confinement layer (Fig.1). The flyer travels across a specific distance to gain the impact velocity that, under optimized conditions, allows the creation of a jet able to break down surface oxides and other contaminants and to verify the conditions necessary for welding. Typically, the welded joint exhibits a ring-like profile [9]. The combination of the laser system parameters (i.e. laser energy and spot size), the choice of the confinement and ablative layers and the travel distance of the flyer as well as its thickness all determine the velocity and the dynamic angle assumed by the flyer during the impact [12]. Generally, a low thickness of the flyer brings to a higher impact speed but implies a lower joint strength [12]. The effect of the flyer's thickness is more marked below specific threshold values determined by welding conditions, including the specifics of the laser system [13]. High surface roughness of the target (in the order of tenths of μm) was found to affect the collision angle and the weldability window [14], as also summarized in [15].

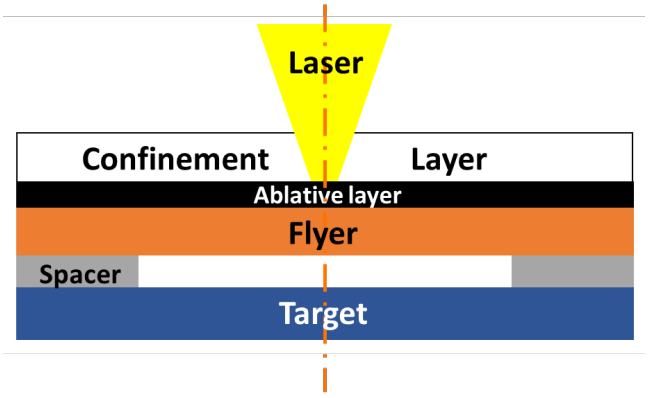

Fig. 1 – Schematic of the laser impact welding process.

Nevertheless, the mentioned processes require in-depth investigation as the final application of interest, i.e. bone fixators, further adds constraints to the materials to be used into the body and their conditions after processing [16]. Also, processes like laser impact welding still feature issues, in particular in terms of the shape of the joints that can be obtained and damage of the flyer and, often, the target, thus requiring extensive experimental campaigns and specific design of the parts to be welded to properly accommodate process constraints [12].

To reduce the effort devoted to extensive experimental testing, both in terms of time and costs, predictive models of the impact welding processes are currently being studied [17] .

This work presents an experimental setup dedicated to employing the laser impact welding process to obtain spot joints between Nickel-Titanium and Magnesium alloy sheets. In parallel, a preliminary finite element model of the process to be used for weldability window prediction has been developed and described.

Methodology

Experimental tests. A commercially available Nd:YAG laser source was used, in a Continuum PowerliteTM Precision II Scientific System. The maximum output energy of the laser is 3.1 J with a pulse width of 8.0 ns, and a wavelength of 1064 nm. The laser system can operate up to a 10 Hz pulse repetition rate or in single shot mode. In this work, a laser energy of 3.1 J was used.

NiTi#1 alloy foils provided by Fort Wayne Metals (IN, USA) with a size or 25 mm x 7 mm and thickness of 250 µm and a customized Mg alloy *Mg-1.2Zn-0.5Ca-0.5Mn* (wt%) foils [18] with a size of 15 mm x 15 mm and a thickness of 200 µm were tested for welding. Welding parameters such as laser spot size and relative distance (stand-off) between flyer and target were varied. In particular two values of the laser spot size were tested: 3.00 mm and 5.22 mm. As stand-off distance, values of 300 and 500 µm have been used.

As suggested in literature [8] the alloy with higher ductility generally outperforms the less ductile material as flyer, thus *Mg* alloy foils were preliminary used as flyer, while *NiTi* alloy foils were used as target. The *NiTi* alloy foils were used in as-rolled conditions while the *Mg* alloy foils were ground up to #1200. Both flyer and target were sonicated in ethanol before welding.

The testing configuration is shown in Fig. 2. Target and flyer are placed on a metallic support (necessary as a support for the thin target [13]) locked on an holder to be located into the welding chamber. Black tape was used as backing to reduce rebound [18].

The stand-off distance between target and flyer was given by metallic ring spacers. The ablative layer in this case is given by a layer of GPN spread upon the flyer and covered by the confinement layer. Borosilicate glass and acrylic, with optimized thickness according to the laser system conditions, were both tested as confinement layers to tune the reaction force on the flyer [12].

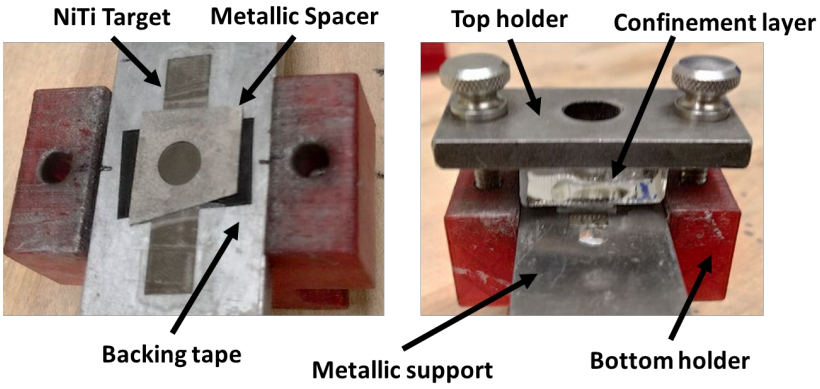

Fig. 2 – Images of the experimental setup for the laser impact welding tests.

Finite Element Model. The numerical procedure was developed through a finite element model of the laser impact welding process using the SFTC Deform 2D® software, simplifying the experimental setup into 2D axisymmetric simulations, given the axisymmetric nature of the welded spot [19] and involving an automatic remeshing routine to handle the large plastic deformation involved. The target and flyer materials were modeled as plastic bodies and divided into 1500 elements each. The average element edge length was about 20 µm. Flow stress data for flyer and target were obtained from [20], considering the high strain rate induced by the process.

The bottom metallic support, spacer and top holder were defined as rigid bodies. The global heat transfer coefficient with the environment was established between the flyer and the target and

it was set equal to 10^5 kW/(m^{2}K) according to literature [21] while no thermal effects due to the plasma have been included in the simulation tests, due to the adiabatic nature of the process demonstrated in [15].

The plasma pressure distribution was simulated according to the equation (1) obtained by Sunny and Gleason et al [17, 23]:

$$p(x) = \frac{1}{\bar{\sigma}\sqrt{2\pi}}\, e^{-\frac{1}{2}(\frac{x}{\bar{\sigma}})^2}. \quad (1)$$

Where x is the radial distance from the spot center (Fig. 3) and $\bar{\sigma}$ represents the standard deviation of the experimental laser intensity distribution [22].

The impact speed on the top surface of the flyer reached right before the impact [10] and the friction at the interface between flyer and target were used as input to the finite element model while the interface temperature on the flyer was analyzed as output. As regards the impact speed, a range of values between 100 m/s and 900 m/s was tested which, based on literature experimental measurements, incorporates in a complex fashion the effects of the travel distance (stand-off), laser parameters set to accelerate the flyer, and the flyer thickness [8]. A 90% fraction of the plastic work was set to be converted to heat [15].

Due to the process characteristics, the friction at the interface between flyer and target was modeled using a constant shear friction based on [23], where the friction factor is defined by equation (2):

$$m = \frac{f_s}{\mathrm{k}}. \quad (2)$$

Being f_s the frictional stress and k the shear yield stress. Values of the friction factor m between 0.1 and 0.3 have been tested [24], with steps of 0.05 since friction plays a pivotal role into local temperatures and process evolution [17]. Table 1 reports a summary of the studied values for impact speed v and friction m while Figure 3 shows the configuration of the finite element model.

Table 1 – Values investigated for friction factor m values and impact speed v.

m [-]	v [m/s]
0.10	100
0.15	200
0.20	300
0.25	600
0.30	900

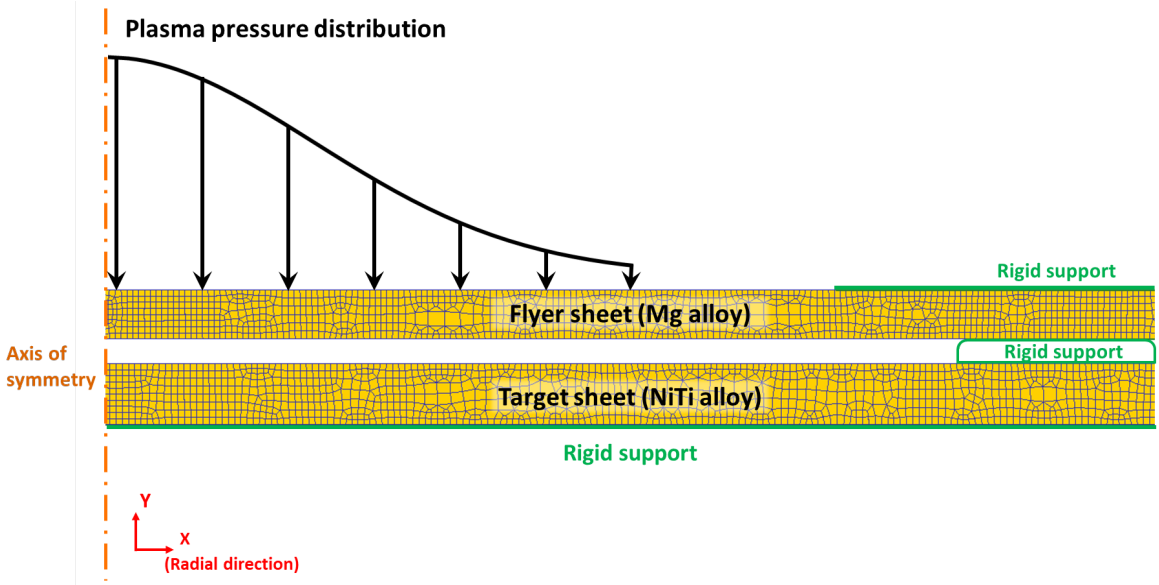

Fig. 3 – Finite Element Model setup on SFTC Deform 2D®.

Results and Discussion

Experimental tests. The experimental campaign carried out confirmed the influence of the confinement layer material on the weld obtainment [8]. In fact, under the tested conditions, using the acrylic material brought to a higher quantity of deposited flyer material onto the target: Fig. 4 shows the successful deposition of the *Mg* alloy flyer onto the surface of the *NiTi* alloy target for a laser spot size of 5.22 mm using acrylic (Fig. 4b) as compared to borosilicate glass (Fig. 4a). Further assessments are necessary by finely tuning laser energy and spot size as less damage to the flyer was reported for increased laser spot size, and by lowering laser beam energy density [13].

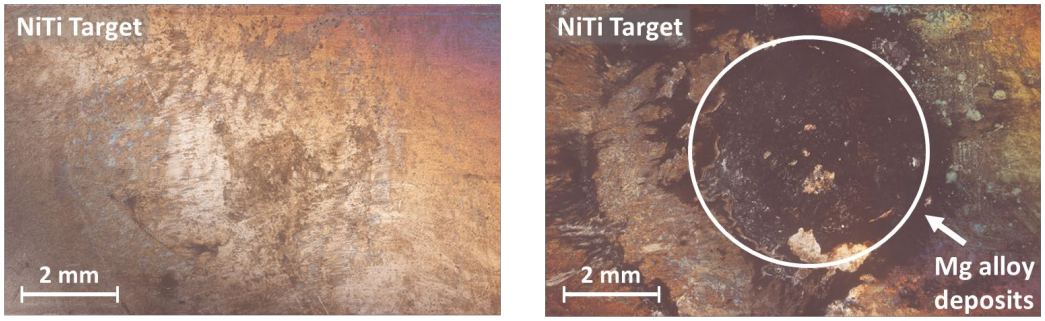

Fig. 4 – Macrographs of the NiTi targets, with varying confinement layer material a) absence of adhered material from the flyer by using borosilicate glass and b) adhered material from the flyer by using acrylic.

Finite Element Model. A range of processing conditions bringing to local melting (around 650 °C [25]) of the *Mg* flyer material was detected at the interface between target and flyer (Fig. 6). This is in accordance with the possible interface melting during the process [8] due to the high plastic deformation and the high strain rates involved in impact welding, together with consequent increase in temperature due to plastic dissipative heating and friction [26]. Local temperature rise might prevent a successful joint if the temperature reached far exceeds the melting temperature of the alloy, thus highlighting the importance to predict the temperature trends.

Extremely high strain rates around 10^6 - 10^7 s^{-1} were obtained for the flyer, as also reported in [18]. The presence of a range where local melting does not occur reflects the possibility to reach

optimum conditions for the process and possibly define a weldability window [9]. Weldability can be defined based on the local stress reached at the interface and related to impact velocity, since bonding has been found to happen within a certain threshold range that varies as a function of the materials to be joined [27].

By both looking at the results in the 3D plot of maximum temperatures in Fig. 5, it is evident that the predictions are sensitive to the coefficient of friction [28], much more than to the impact velocity. Thus, highlighting the relevance of a correct estimation of the friction factor for the proper calibration of the model, being friction related to multiple factors such as cleanliness of the surfaces, oxides, local temperature and pressure conditions [29].

Fig. 6 shows the temperature distribution on the flyer for the conditions v 100 m/s and m 0.10, at the interface with the target, highlighting a maximum along a ring having the size of the laser spot. The significant rise in the temperature of the flyer was located within tenths of μm distance from the interface with the target.

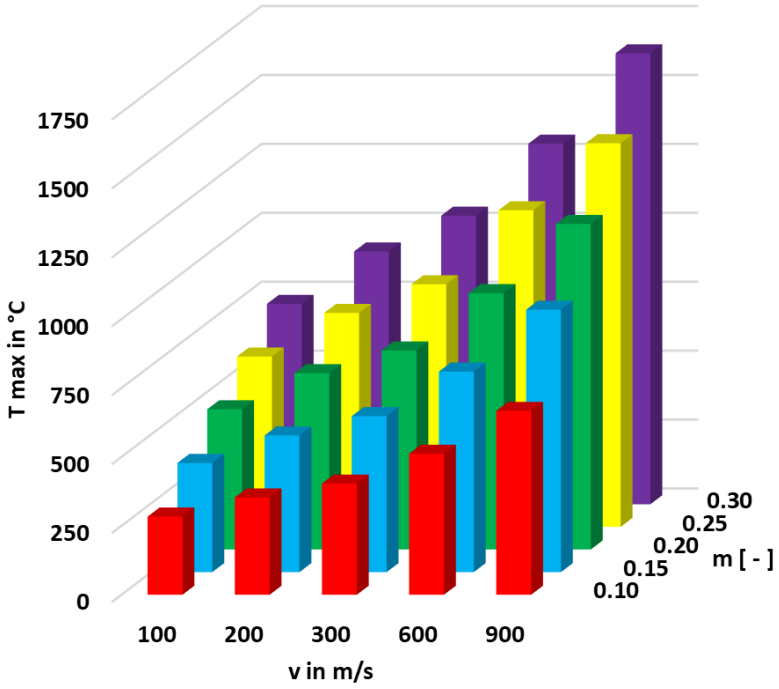

Fig. 5 – 3D plot of maximum temperature reached on the Mg flyer at the flyer-target interface.

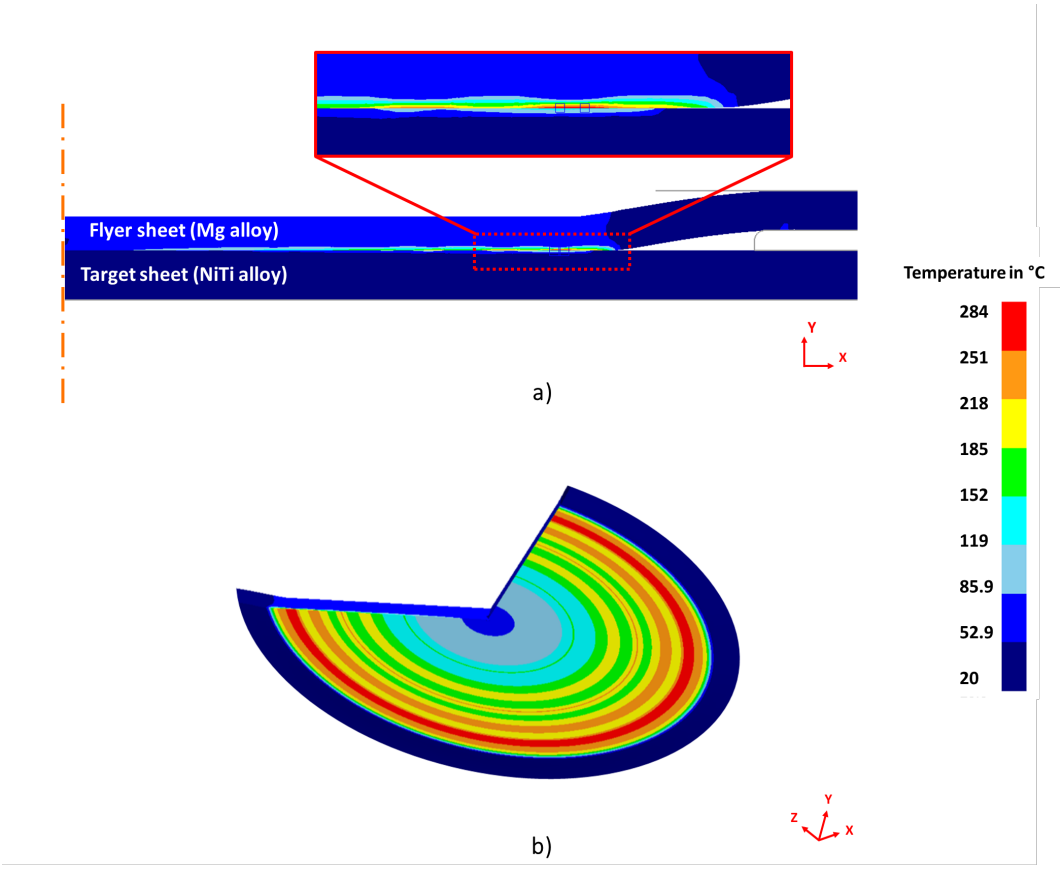

Fig. 6 – Maximum temperature reached on the Mg flyer at the flyer-target interface for the configuration at v 100 m/s and m 0.10 (a) 2D view, (b) 3D view.

Summary and Outlook

The current work showed a parallel development of both experimental and numerical testing configurations for the joining of *NiTi* and *Mg* alloys towards the development of multi-material skeletal fixation devices. From an experimental point of view, preliminary results confirm the possibility to deposit *Mg* alloys on *NiTi* alloys as also anticipated from the literature. Nevertheless, the whole testing process involves a great amount of trials in order to locate a possible weldability window, able to preserve both flyer integrity and prevent local melting and materials mixing at the weld interface. The finite element modeling shows promising results in terms of accordance with literature trends.

Future development will involve the calibration of the model to be used as a predictive tool for future experimental campaigns. Modeling aspects concerning the effects of materials flow stress - also including the effects of alloying elements -, materials damage, welding criteria based on local stress increase as studied in [30] will be then included. Measurement of the experimental values of the impact velocity will also be addressed to connect experimental and simulation results.

References

[1] A. Chmielewska and D. Dean, The role of stiffness-matching in avoiding stress shielding-induced bone loss and stress concentration-induced skeletal reconstruction device failure. Acta Biomater. 173. 51–65. (Jan. 2024). https://doi.org/10.1016/j.actbio.2023.11.011

[2] M. S. Gogheri, M. Kasiri-Asgarani, H. R. Bakhsheshi-Rad, H. Ghayour, and M. Rafiei, Mechanical properties, corrosion behavior and biocompatibility of orthopedic pure titanium−magnesium alloy screw prepared by friction welding. Trans. Nonferrous Met. Soc. China

(English Ed. 30 (11). 2952–2966. (2020). https://doi.org/10.1016/S1003-6326(20)65434-6

[3] A. Chmielewska, A. Luo, B. Panton, L. Olivas, and D. Dean, Multimaterial Stiffness-Matched Implants (US Provisional Patent Application)

[4] N. Gangil, A. N. Siddiquee, S. Mufazzal, S. M. Muzakkir, and S. Maheshwari, Shape memory alloy based NiTi reinforced functionally graded material for vibration damping. Proc. Inst. Mech. Eng. Part L J. Mater. Des. Appl. 235 (12). 2771–2782. (2021). https://doi.org/10.1177/14644207211035521

[5] S. Ji, W. Hu, Z. Ma, Q. Li, and X. Gong, Friction Stir Lap Welding of Mg/Ti Dissimilar Alloys Using a Slight Penetration Depth. JOM. 72 (4). 1589–1596. (Apr. 2020). https://doi.org/10.1007/s11837-019-03959-x

[6] M. Sen, S. Shankar, and S. Chattopadhyaya, Micro-friction stir welding (μFSW) – A review. Mater. Today Proc. 27. 2469–2473. (2020). https://doi.org/10.1016/j.matpr.2019.09.220

[7] A. Shamsolhodaei, J. P. Oliveira, B. Panton, B. Ballesteros, N. Schell, and Y. N. Zhou, Superelasticity preservation in dissimilar joint of NiTi shape memory alloy to biomedical PtIr. Materialia. 16 (November 2020). 101090. (2021). https://doi.org/10.1016/j.mtla.2021.101090

[8] W. Cai *et al.*, A state-of-the-art review on solid-state metal joining. J. Manuf. Sci. Eng. Trans. ASME. 141 (3). (2019). https://doi.org/10.1115/1.4041182

[9] H. Wang and Y. Wang, High-velocity impact welding process: A review. Metals (Basel). 9 (2). (2019). https://doi.org/10.3390/met9020144

[10] F. Du, L. Deng, X. Wang, M. Zhang, J. Jin, and J. Zhang, Study on interfacial characteristics and properties of NiTi/Al–Mg joint by vaporizing foil actuator welding. J. Mater. Res. Technol. 20. 3429–3440. (Sep. 2022). https://doi.org/10.1016/j.jmrt.2022.08.090

[11] J. Li, B. Panton, S. Liang, A. Vivek, and G. Daehn, High strength welding of NiTi and stainless steel by impact: Process, structure and properties. Mater. Today Commun. 25 (March). 101306. (2020). https://doi.org/10.1016/j.mtcomm.2020.101306

[12] K. Wang, H. Wang, H. Zhou, W. Zheng, and A. Xu, Research status and prospect of laser impact welding. Metals (Basel). 10 (11). 1–18. (2020). https://doi.org/10.3390/met10111444

[13] H. Wang, A. Vivek, Y. Wang, G. Taber, and G. S. Daehn, Laser impact welding application in joining aluminum to titanium. J. Laser Appl. 28 (3). (2016). https://doi.org/10.2351/1.4946887

[14] J. Bellmann *et al.*, Particle Ejection by Jetting and Related Effects in Impact Welding Processes. Metals (Basel). 10 (8). (2020). https://doi.org/10.3390/met10081108

[15] G. Gleason, K. Bailey, S. Sunny, A. Malik, and R. A. Bernal, Influence of surface roughness on the transient interfacial phenomena in laser impact welding. J. Manuf. Process. 80 (February). 480–490. (2022). https://doi.org/10.1016/j.jmapro.2022.06.022

[16] W. R. Wagner, S. E. Sakiyama-Elbert, G. Zhang, and M. J. Yaszemski, Biomaterials Science: An Introduction to Materials in Medicine. 2020. https://doi.org/10.1016/C2017-0-02323-6

[17] A. Nassiri, G. Chini, A. Vivek, G. Daehn, and B. Kinsey, Arbitrary Lagrangian-Eulerian finite element simulation and experimental investigation of wavy interfacial morphology during high velocity impact welding. Mater. Des. 88. 345–358. (2015). https://doi.org/10.1016/j.matdes.2015.09.005

[18] S. Sadeh *et al.*, Simulation and experimental comparison of laser impact welding with a

plasma pressure model. Metals (Basel). 9 (11). (2019). https://doi.org/10.3390/met9111196

[19] X. Wang, H. Zhang, Z. Shen, J. Li, Q. Qian, and H. Liu, Experimental and numerical investigation of laser shock synchronous welding and forming of Copper/Aluminum. Opt. Lasers Eng. 86. 291–302. (Nov. 2016). https://doi.org/10.1016/j.optlaseng.2016.06.018

[20] Y. V. R. K. Prasad, K. P. Rao, and S. Sasidhara, Hot Working Guide: A Compendium of Processing Maps. Second. ASM International, 2015. [Online]. Available: http://linkinghub.elsevier.com/retrieve/pii/B978008033454750019X

[21] P. J. Arrazola, T. Özel, D. Umbrello, M. Davies, and I. S. Jawahir, Recent advances in modelling of metal machining processes. CIRP Ann. - Manuf. Technol. 62 (2). 695–718. (2013). https://doi.org/10.1016/j.cirp.2013.05.006

[22] G. Gleason, S. Sunny, S. Sadeh, H. Yu, and A. Malik, Eulerian modeling of plasma-pressure driven laser impact weld processes. Procedia Manuf. 48 (2019). 204–214. (2020). https://doi.org/10.1016/j.promfg.2020.05.039

[23] S. Kalpakjian and S. R. Schmid, Tecnologia Meccanica. Sixth. Pearson, 2021.

[24] O. Majidi, M. Jahazi, and N. Bombardier, Finite element simulation of high-speed blow forming of an automotive component. Metals (Basel). 8 (11). (2018). https://doi.org/10.3390/met8110901

[25] M. M. Avedesian and H. Baker, Eds., ASM Specialty Handbook: Magnesium and Magnesium Alloys. ASM International, 1999.

[26] J. L. Robinson, The mechanics of wave formation in impact welding. Philos. Mag. A J. Theor. Exp. Appl. Phys. 31 (3). 587–597. (Mar. 1975). https://doi.org/10.1080/14786437508226540

[27] H. Wang, D. Liu, J. C. Lippold, and G. S. Daehn, Laser impact welding for joining similar and dissimilar metal combinations with various target configurations. J. Mater. Process. Tech. 278 (November 2019). 116498. (2020). https://doi.org/10.1016/j.jmatprotec.2019.116498

[28] T. Lee, A. Nassiri, T. Dittrich, A. Vivek, and G. Daehn, Microstructure development in impact welding of a model system. Scr. Mater. 178. 203–206. (2020). https://doi.org/10.1016/j.scriptamat.2019.11.031

[29] B. Bhushan, Introduction to tribology. Second Edi. John Wiley & Sons, Ltd., 2013.

[30] F. Gagliardi, T. Citrea, G. Ambrogio, and L. Filice, Influence of the process setup on the microstructure and mechanical properties evolution in porthole die extrusion. Mater. Des. 60. 274–281. (2014). https://doi.org/10.1016/j.matdes.2014.04.004